Redox Biology 62 (2023) 102684

Contents lists available at ScienceDirect

Redox Biology

journal homepage: www.elsevier.com/locate/redox

miR-484 mediates oxidative stress-induced ovarian dysfunction and promotes granulosa cell apoptosis via SESN2 downregulation

Xiaofei Wang [a], Jiahao Yang [a], Huiying Li [a], Hongbei Mu [a], Ling Zeng [c], Siying Cai [a], Ping Su [a,b], Huaibiao Li [a,**], Ling Zhang [a,b,***], Wenpei Xiang [a,b,*]

[a] Institute of Reproductive Health, Tongji Medical College, Huazhong University of Science and Technology, 13 Hangkong Road, Wuhan, 430030, China
[b] Wuhan Huake Reproductive Hospital, 128 Sanyang Road, Wuhan, 430013, China
[c] Medical Genetics Center, Maternal and Child Health Hospital of Hubei Province, Wuhan, 430070, China

ARTICLE INFO

Keywords:
miR-484
Oxidative stress
Granulosa cells
Ovarian dysfunction
Mitochondria
Apoptosis

ABSTRACT

Ovarian dysfunction is a common cause of female infertility, which is associated with genetic, autoimmune and environmental factors. Granulosa cells (GCs) constitute the largest cell population of ovarian follicles. Changes in GCs, including oxidative stress (OS) and excessive reactive oxygen species (ROS), are involved in regulating ovary function. miR-484 is highly expressed in 3-NP-induced oxidative stress models of ovaries and GCs. miR-484 overexpression aggravated GCs dysfunction and thereby intensified ovarian oxidative stress injury in mice. Moreover, bioinformatic analyses, luciferase assays and pull-down assays indicated that LINC00958 acted as a competing endogenous RNA (ceRNA) for miR-484 and formed a signaling axis with Sestrin2(SESN2) under oxidative stress conditions, which in turn regulated mitochondrial functions and mitochondrial-related apoptosis in GCs. Additionally, the inhibition of miR-484 alleviated GCs dysfunction under ovarian oxidative stress condition. Our present study revealed the role of miR-484 in oxidative stress of ovaries and GCs and the function of LINC00958/miR-484/SESN2 axis in mitochondrial function and mitochondria-related apoptosis.

1. Introduction

According to World Health Organization's estimation, infertility will become the third largest disease in the 21st century following tumors and cardiovascular diseases, affecting almost 45 million couples worldwide [1,2]. The incidence of infertility is currently increasing and it is estimated that 10%–15% of couples in China are infertile, with male and female factors contributing equally [3,4]. Several factors have been proved to cause women's infertility; age, genetic factors, immune factors, unhealthy lifestyle and environmental pollution have received widespread attention over the past few decades [5,6].

Ovarian granulosa cells (GCs) are one of the key components of the follicular microenvironment, which communicate directly with oocytes through gap junctions. Their interaction with oocytes determines the quality of follicle development, female fertility and the outcome of assisted reproductive technologies [7–9]. Changes in the follicular microenvironment, including oxidative stress (OS) and excessive reactive oxygen species (ROS), are important pathological factors which may affect ovary function and induce female infertility [10,11]. According to recent studies, excessive oxidative stress in GCs can impose negative effects on follicle development, oocyte maturation and ovulation, affect ovarian reserve and even lead to female infertility [12,13].

The miRNA is a small non-coding RNA (19-22 nt) which acts as a post-transcriptional regulator of gene expression in various biological processes including proliferation, oxidative stress, inflammation, apoptosis and angiogenesis. miRNAs are a key regulator to multiple ovarian diseases, such as premature ovarian failure (POF), endometriosis, ovarian inflammation and ovarian tumors [14–16]. The miRNA-mRNA interaction network participates in the regulation of oxidative stress induced GCs injury. Te Liu et al. found that miR-15b can induce premature ovarian failure in mice by inhibiting the expression of α-Klotho in GCs [17]. Therefore, searching for the key miRNAs

Abbreviations: 3-NP, 3-nitropropionic acid; OS, oxidative stress; ROS, reactive oxygen species; GCs, granulosa cells.

* Corresponding author. Wuhan Huake Reproductive Hospital, 128 Sanyang Road, Wuhan, 430013, China.
** Corresponding author.
*** Corresponding author. Institute of Reproductive Health, Tongji Medical College, Huazhong University of Science and Technology, 13 Hangkong Road, Wuhan, 430030, China.
E-mail addresses: lihuaibiao@hust.edu.cn (H. Li), Zhling312@163.com (L. Zhang), wpxiang2010@hust.edu.cn (W. Xiang).

https://doi.org/10.1016/j.redox.2023.102684
Received 19 February 2023; Received in revised form 15 March 2023; Accepted 17 March 2023
Available online 20 March 2023

regulating the oxidative stress of GCs and revealing its mechanisms are of great value for further clarifying the pathophysiological mechanisms underlying female infertility and screening therapeutic targets in the future.

miR-484 is a newly discovered non-coding RNA which has been reported to be closely related to mitochondrial fission and fusion. Wang K and other researchers have found that miR-484 directly targets Fis1 to regulate cardiomyocyte apoptosis [18]. Our previous study found that miR-484 was significantly increased in follicular fluid-derived GCs in patients who were diagnosed as diminished ovarian reserve (DOR), suggesting that miR-484 is relevant to ovarian reserve [19]. However, it is not clear whether miR-484 mediates GCs oxidative stress in the regulation of ovarian reserve dysfunction.

The present study aims to unveil the role and mechanism of miR-484 in regulating oxidative stress in GCs, therefore providing a theoretical basis for improving the GCs function and alleviating ovarian oxidative stress to ameliorate ovarian dysfunction.

2. Materials and methods

2.1. Animals and experimental design

2.1.1. The 3-NP-induced OS model of mouse establishment

Eight-week-old female C57BL/6J mice were purchased from Beijing Vital River Laboratory Animal Technology Co., Ltd and fed with standard food and water. All animal procedures and protocols were approved by the Institutional Animal Care and Use Committee of Tongji Medical College, Huazhong University of Science and Technology (IACUC number: S2564). In brief, 40 female C57BL/6J mice were randomly divided into two groups: (1) Control group; (2) OS (oxidative stress) group. The OS group, which received intraperitoneal injection with 20 mg/kg 3-nitropropionic acid (3-NP, Sigma, USA) diluted with phosphate-buffered saline (PBS, Procell, China) once a day for 2 weeks, whereas the control group, which received an equal volume of PBS. The mode and dose of administration were chosen based on previous studies [20–22].

2.1.2. AAV administration intra-ovarian injection

The mice were injected with 1.17E+13 VG/mL adeno-associated virus 9 (AAV9) containing miR-484-specific small hairpin RNA (miR-484 inhibitor) via intra-ovarian injection to establish an ovary-specific miR-484 knockdown model. Likewise, mice received treatment of Flag-tagged AAV9(AAV vector) served as the control group. There are five groups, including the Control, OS, OS + AAV-vector, OS + AAV-inhibitor, and OS + Melatonin, and Melatonin (MCE, USA) was used as positive controls.

2.2. Oxidative stress and ROS measurement

The level of Malondialdehyde (MDA) was determined using an MDA Assay Kit. The activities of Total Superoxide Dismutase (SOD) and Glutathione Peroxidase (GSH-Px) were analyzed with SOD and GSH-Px Activity Assay Kits. All kits used were purchased from Nanjing Jiancheng Bioengineering Institute. The level of ovarian ROS was measured by a ROS assay kit using DHE probe (Solarbio, China, BC1295). The level of intracellular ROS was measured by a ROS assay kit using DCFH-DA probe (Beyotime, China, S0033S). A MitoSOX Red Mitochondrial Superoxide Indicator (Invitrogen, USA, M36008) was used to quantify mitochondrial ROS (mtROS) production. Briefly, GCs were rinsed and incubated with the fluorescent probe in the dark at 37 °C for 25 min. The images were captured using a ZEISS confocal microscope (LSM900, Germany). The intracellular ROS and mtROS content were expressed as the area of intensity (AOI).

2.3. Fluorescence in situ hybridization (FISH)

The specific FISH probes to miR-484 and LINC00958 were designed and synthesized by Wuhan Servicebio Biotechnology Co. The hybridization was performed by commercial FISH Kit (RiboBio, China) as previously reported [19].

2.4. Paraffin embedding and hematoxylin-eosin staining

Mouse ovaries were sectioned after fixation and dehydration with 4% paraformaldehyde. Hematoxylin eosin staining was performed as previously reported [23].

2.5. Immunofluorescent staining

Paraffin-embedded sections were blocked with QuickBlock (Beyotime, China) for 1 h and then stained with an anti-Ki67 antibody (Proteintech, China) and a secondary antibody (Proteintech, China). Finally, the images were captured with a ZEISS Confocal Microscope (LSM 900, Germany).

2.6. Serum hormone test

Reagent kits for the anti-Müllerian hormone (AMH), estradiol (E2) and follicle-stimulating hormone (FSH) were purchased from Shanghai Enzyme-linked Biotechnology Co., Ltd. (Shanghai, China). These assays were performed following the manufacturer's instructions.

2.7. Measurement of estrous cycle

Mouse estrous cycle phase was determined by observing vaginal mucus smear. Briefly, a cotton swab was moistened with saline, inserted into the vagina then coated on a slide. Then, the vaginal smears were stained with Giemsa staining and examined for histological changes under an Olympus microscope. The images of each cycle were diagnosed based on the previous literature [24].

2.8. TUNEL apoptosis assay

A TUNEL Apoptosis Assay Kit (Abbkine, China) was used to evaluate TUNEL-positive sections in mouse ovaries. Briefly, ovarian slices were fixed with 4% paraformaldehyde then stained with TUNEL detection solution in the dark for 1h. The fluorescent images were captured with ZEISS Confocal Microscope (LSM 900, Germany).

2.9. RNA extraction and quantitative real-time PCR (RT-qPCR)

RNA extraction was performed using RNA-easy Isolation Reagent (Vazyme, China) based on the manufacturer's instructions. The quantitative expression of LINC00958, miR-484, SESN2 and other mRNAs was detected by the AceQ qPCR SYBR Green Master Mix (Vazyme, China). The $2^{-\Delta\Delta CT}$ method was used to calculated the relative gene expression level. The primers used in the study are showed in Table S1.

2.10. Preparation of the cytoplasmic and mitochondrial fractions

Cell Mitochondria Isolation Kit was used to separate cytoplasm and mitochondria proteins in accordance with the manufacturer's instructions. Samples of cytosol and mitochondria were dissolved in lyses buffer and proteins were subjected to Western blotting respectively.

2.11. Western blot assay (WB)

Total proteins from GCs were extracted by RIPA Lysis and Extraction Buffer (Thermo Fisher, USA). After separated by SDS-PAGE electrophoresis, proteins were transferred to PVDF membranes and blocked

with Blocking Buffer (Beyotime, China). Following incubation with primary antibodies against BAX (Proteintech, China), BCL2 (Abmart, China), Cleaved Caspase-3 (CST, USA), cytochrome *c* (Abcam, UK), FOXO1 (Proteintech, China), SIRT1 (Proteintech, China),AMPKα(CST, USA), SOD2 (Proteintech, China), SESN2 (Abcam, UK), NF-κB (Abmart, China),PGC1α(Proteintech, China),FIS1(Proteintech, China), YAP1 (CST, USA), and β-actin (Proteintech, China) in Trisbuffered saline (TBS) containing 0.1% Tween-20 (TBST) at 4 °C overnight, HRP-conjugated secondary antibodies and ECL HRP Substrate were used to visualize the protein bands according to our previous study [19].

2.12. Culture and identification of GCs

Human ovarian granulosa cell line SVOG was purchased from Shanghai Hongshun Biotechnology Co., LTD. The GCs were cultured in T25 flasks (NEST, China) with DMEM high glucose medium containing 10% FBS and 1% penicptomycin. The GCs was identified by FSHR immunofluorescent staining (Proteintech; China) according to our previous study [19].

2.13. Cell treatment

To mimic oxidative stress in GCs, cells were treated with 3-NP (Sigma, USA) at the dosage of 0, 0.25, 0.5, 1, 2.5, 5, 10, and 20 mM in 48-well plates for 24 h. Short interfering RNA for LINC00958 (si1-LINC00958, si2-LINC00958 and si3-LINC00958), short interfering RNA for SESN2 (si1-SESN2, si2-SESN2 and si3-SESN2), miR-484 mimic and its negative control (mimic-NC), miR-484 inhibitor and its negative control (inhibitor-NC) were purchased from RiboBio and genomeditech Biotechnology Co., LTD. The SESN2 overexpression plasmid and its

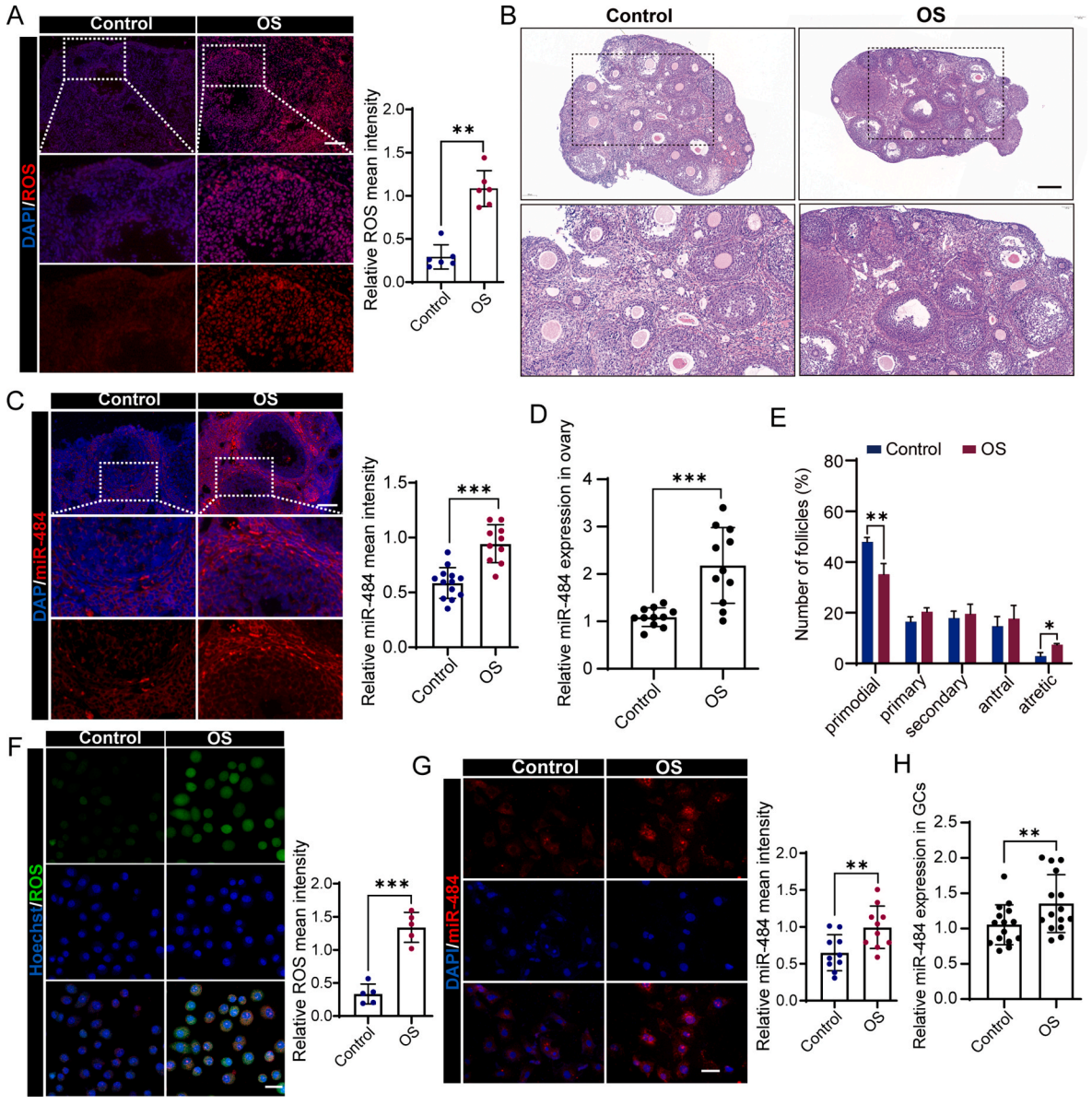

Fig. 1. miR-484 is highly expressed in 3-NP-induced oxidative stress (OS) models of ovaries and GCs. (A) Ovarian ROS levels of C57BL/6J mice were measured using DHE probe in the Control and OS group after 2 weeks of PBS or 3-NP treatment (n = 6). Scale bar, 50 μm. (B) H&E staining to show ovarian structures in the Control and OS group and (E) the number of follicles was quantified for each group (n = 5). Scale bar, 500 μm. (C–D) The expression levels of miR-484 in ovarian tissues in the Control and OS group were determined using FISH and RT-qPCR (n ≥ 10). Scale bar, 50 μm. (F) Intercellular ROS contents of GCs (SVOG cells) were measured using DCFH-DA probe and quantified in the Control and OS group for PBS or 10 mM 3-NP treatment for 24h (n = 5). Scale bar, 50 μm. (G–H) The expression levels of miR-484 in ovarian tissues in the Control and OS group were determined using FISH and RT-qPCR. (n ≥ 10). Scale bar, 20 μm. Data represent the mean ± SD. *, $P < 0.05$; **, $P < 0.01$; ***, $P < 0.001$.

negative control (OE-control) were constructed by genomeditech (China). The transfection of DNA or RNA in GCs was performed using LipoFectMax™ 3000 Transfection Reagent (ABP Biosciences, USA) at 70% confluence according to the manufacturer's instructions.

2.14. Cell viability assay

Cell Counting Kit-8 assay (Abbkine, China) was used to determine the cell viability. In brief, GCs were incubated with 200 μl working reagent for 1 h in 48-well plates (NEST, China). The optical absorbance at 450 nm of each well was measured with a luminescence microplate reader (Biotek, USA).

2.15. Flow cytometry

To detect apoptosis, the GCs were stained with both Annexin V-FITC/PI (Abbkine, China). The percentages of early apoptotic cells and late apoptotic cells were measured with a flowcytometry system (BD BioSciences, USA)

2.16. EdU staining assay

The GCs were cultured in 50 μM EdU containg medium for 2 h, and then fixed with 4% paraformaldehyde for 30 min. After incubated with 2 mg/ml glycine and permeabilized with 0.2% Triton X-100, the GCs were stained with DAPI for nuclear staining. The fluorescent images were captured with ZEISS Confocal Microscope (LSM 900, Germany). Cell proliferation was analyzed by assessing the percentage of EdU-positive cells.

2.17. Measurement of mitochondrial function and endoplasmic reticulum (ER) function

Mitochondrial morphology, mtochondrial membrane potential (MMP) depolarization, ATP levels and ER specific fluorescence staining were assessed by MitoTracker Red (Beyotime, China), JC-1 assay kit (Beyotime, China), ATP Assay Kit (Beyotime, China) and ER-Tracker Red (Beyotime, China) following the manufacturer's instructions, respectively.

2.18. Luciferase reporter assay

The 3′-UTR of LINC00958 and SESN2 contain conserved miR-484 binding sites. QuikChange II XL Site-Directed Mutagenesis Kit (Stratagene) was used to synthesize the mutated fragment of 3′-UTR of LINC00958 and SESN2. The luciferase activity assays were performed in transiently transfected HEK-293T cells, the luciferase activity were assessed using the Dual Luciferase Reporter Assay kit (Promega) as previously described [19].

2.19. Pull-down assay

Biotin-labeled miR-484 and biotin-labeled LINC00958 were synthesized using Pierce RNA 3′ End Desthiobiotinylation Kit (Thermo Fisher, USA). After incubated with the GCs lysates with streptavidin-coated magnetic beads using Pierce™ Magnetic RNA-Protein Pull-Down Kit (Thermo Fisher, USA) following the manufacturer's recommendation, the binding RNAs were isolated by TRIzol and analyzed by RT-qPCR.

2.20. RNA immunoprecipitation (RIP)

The GCs were cultured in 10 cm dishes (NEST, China) and transfected with miR-484 mimic and mimic-NC. AGO2-RIP was performed as previously published studies [25,26]. Briefly, transfected cells were collected by centrifugation and then lysed in lysis buffer and incubated with BeyoMag™ Protein G Plus Magnetic Beads (Beyotime, China) for 2 h at 4 °C. 10% lysates were used as the input and the remained lysates were incubated with Protein G Magnetic Beads conjugated with anti-AGO2 (Abmart, China) or anti-IgG (Beyotime, China) antibodies overnight at 4 °C. After that, the protein components were extracted and RNAs were isolated using TRIzol and Chloroform. The purified RNA was determined by RT-qPCR.

2.21. Statistical analysis

The differences between the two groups were analyzed by the student's *t*-test using GraphPad Prism8 statistical software. $N \geq 3$ biologically independent samples Data. were presented as mean ± SD. $P < 0.05$ was considered as statistically significant.

3. Results

3.1. miR-484 is highly expressed in 3-NP-induced oxidative stress models of ovaries and GCs

miR-484 has been reported to be highly expressed in GCs from DOR patients in our previous study [19]. To investigate the exact expression level of miR-484 in ovaries and GCs after oxidative stress exposure, we used 3-nitropropionic acid (3-NP) to simulate the OS state of ovaries and GCs. 3-NP is an inhibitor of mitochondrial complex II, which can induce mitochondrial production and release of ROS, thus causing oxidative stress.

We successfully established an ovarian oxidative stress model, in which the 3NP-treated mice in the OS group had reduced body weights, shortened estrus period, longer metoestrus period, decreased ovary-to-body-weight ratio and significantly reduced estradiol and AMH levels (Figs. S1A, B, C, D). Specifically, the results showed that the OS group exhibited an increase in ROS levels and MDA levels, as well as a decrease in SOD activity and GSH-Px levels (Fig. 1A and Fig. S1E).

As shown in Fig. 1B and E, the follicles at all developmental stages could be found in the control group, and the GCs were arranged regularly, whereas the OS group showed increased fibrosis, increased atretic follicles and decreased primordial follicles. Next, we evaluated the status of GCs by TUNEL and Ki-67 staining. Compared with the control group, TUNEL-positive cells were increased and Ki-67 positive cells were significantly decreased in the OS group, indicating that GCs apoptosis was aggravated and the proliferative ability was impaired (Figs. S1F and G).

Subsequently, FISH and fluorescence quantitative PCR were used to detect the expression level of miR-484 in ovaries under oxidative stress conditions. The results showed that miR-484 was significantly increased in the OS group in comparison to that in the control group (Fig. 1C and D), which is consistent with our expectations.

To provide more evidence for the upregulation of miR-484 in GCs under oxidative stress conditions, we similarly established an in vitro model of oxidative stress in granulosa cell line SVOG using 3NP treatment. As shown in Fig. S2A, the SVOG cells were identified by detecting the expression of the specific GCs marker FSHR. By referring to the concentration of 3NP used in previous studies [27], we finally determined the concentration of 3-NP as 10 mM for subsequent experiments (Fig. S2B).

Compared with the control group, the intracellular ROS contents and the oxidative stress levels were increased, the antioxidant levels were decreased in the OS group (Fig. 1F, Figs. S2C and D). Furthermore, the results of flow cytometry and EdU proliferative assay showed that the apoptotic level of GCs was increased and the level of cell proliferation was decreased in the OS group, which were consistent with the results of in vivo experiments (Fig. S2E, Fig. S2F). We then examined the expression level of miR-484 in GCs. As a result, miR-484 is highly expressed in GCs after oxidative stress exposure (Fig. 1G and H).

Collectively, these data demonstrated that miR-484 is significantly increased in 3-NP-induced oxidative stress models of ovaries and GCs.

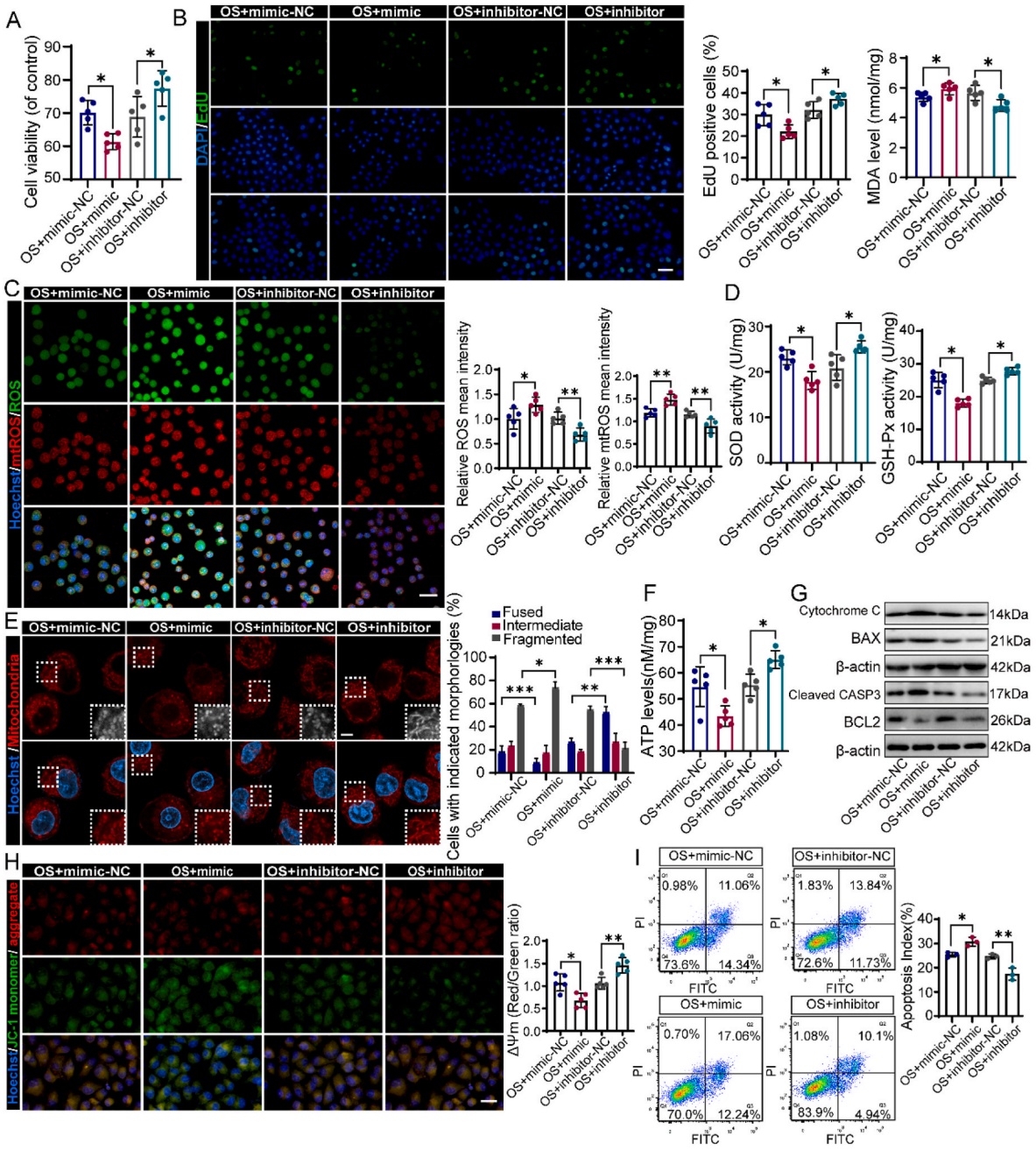

Fig. 2. Overexpression of miR-484 compromised GCs function by damaging mitochondrial functions and increasing apoptosis under oxidative stress conditions. (A) CCK-8 assays were performed to measure the cell viability in silenced- or overexpressed-miR-484 in GCs under oxidative stress (n = 5). (B) EdU assays of GCs and the percentage of EdU-positive GCs (Green) were measured (n = 5). Scale bar, 100 μm. (C) Cellular ROS (Green) and mtROS (Red) in GCs were assessed using DCFH-DA probe and MitoSOX Red mitochondrial superoxide indicator (n = 5). Scale bar, 50 μm. (D) The MDA level and total SOD and GSH-Px activities of GCs (n = 5). (E) MitoTracker (red) was used to stain mitochondria, and mitochondrial morphology is counted (n = 5). Scale bar, 10 μm. (F) ATP levels were recorded following miR-484 knockdown or overexpression in GCs under oxidative stress (n = 5). (G) Western blot was used to measure the expression of apoptosis-associated proteins in GCs. (H) Mitochondrial membrane potential (MMP, ΔΨm) was measured by the JC-1 staining (n = 5). Scale bar, 50 μm. (I) Apoptotic cells were measured by flow cytometry in GCs (n = 3). Data represent the mean ± SD. *, $P < 0.05$; **, $P < 0.01$; ***, $P < 0.001$. (For interpretation of the references to colour in this figure legend, the reader is referred to the Web version of this article.)

3.2. Overexpression of miR-484 compromised GCs function by damaging mitochondrial functions and increasing apoptosis under oxidative stress conditions

To further explored the role of miR-484 in GCs under oxidative stress conditions, miR-484 was overexpressed or inhibited in GCs. GCs were transfected with Cy3-labeled miR-484 mimic at different concentrations for different periods of time. Eventually we chose to transfect the GCs with 100 nM of miR-484 mimics for 24 h for subsequent experiments (Fig. S2G). After oxidative stress injury, miR-484 mimic obviously reduced cell viability and proliferative ability (Fig. 2A and B). In contrast, miR-484 inhibitor led to the opposite results (Fig. 2A and B). Additionally, miR-484 overexpression aggravated oxidative stress injury, as shown by the reduced SOD activities, decreased GSH-Px levels, elevated cellular ROS and mtROS levels, and MDA levels (Fig. 2C and D). The opposite trend was observed in miR-484 depleted GCs (Fig. 2C and

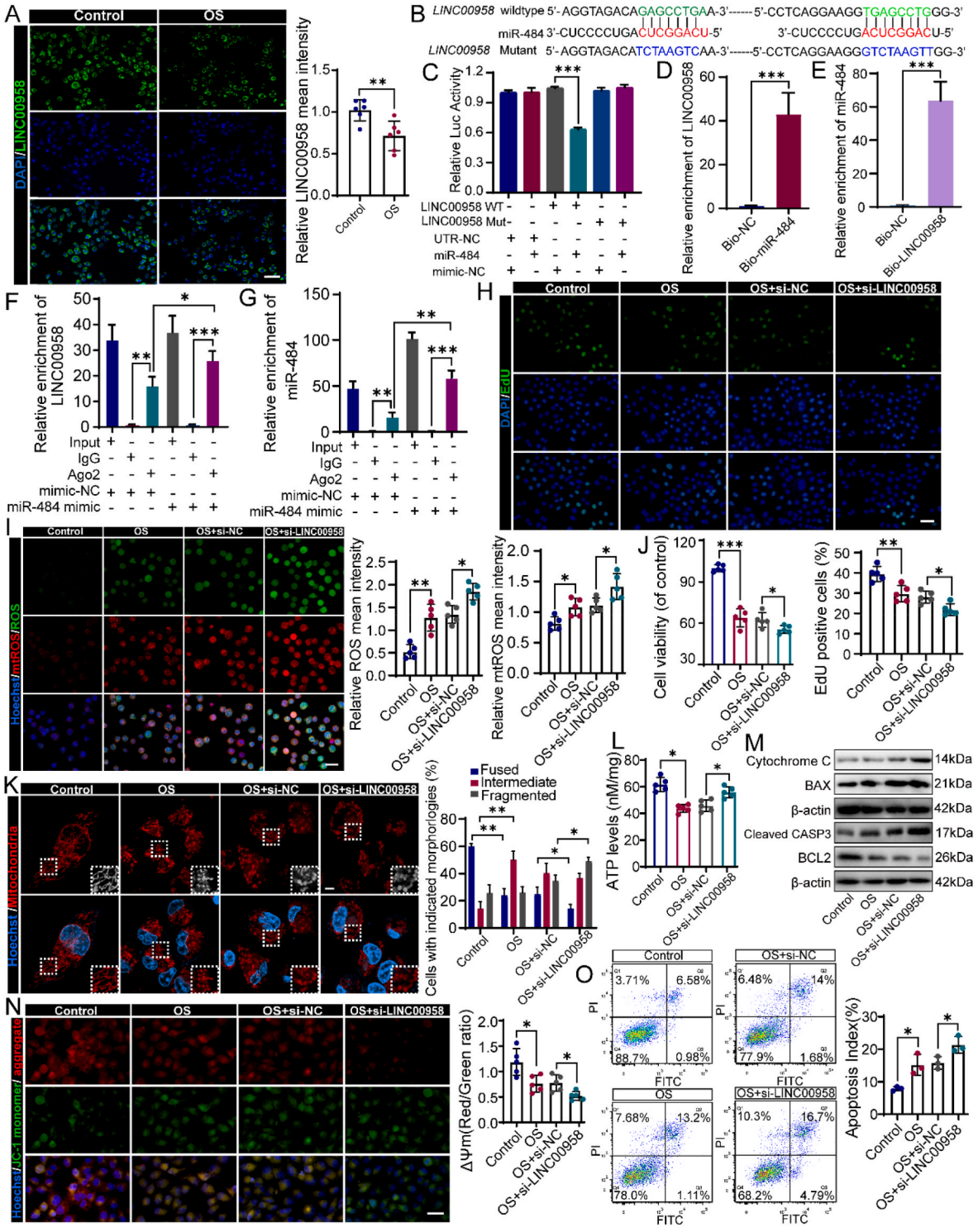

Fig. 3. Prediction and confirmation of direct interaction between miR-484 and LINC00958 in GCs. (A) FISH was performed to detect the expression of LINC00958 in the Control and OS group (n = 6). Scale bar, 50 μm. (B–C) The predicted binding sites of LINC00958 and miR-484 and the luciferase reporter assay showed direct binding between the LINC00958-WT and the miR-484. (D–E) GCs were transfected with biotinylated wild-type miR-484 or biotinylated LINC00958. RNA pull-down assay showed that LINC00958 was associated with miR-484. (F–G) The RIP assay for LINC00958 was performed with an anti-AGO2 antibody in GCs transfected with miR-484 mimics or mimic-NC, and the expression of LINC00958 and miR-484 was measured. (H) EdU assays of GCs and the percentage of EdU-positive GCs (Green) were measured (n = 5). Scale bar, 100 μm. (I) Cellular ROS (Green) and mtROS (Red) in GCs were assessed using DCFH-DA probe and MitoSOX Red mitochondrial superoxide indicator (n = 5). Scale bar, 50 μm. (J) CCK-8 assays were performed to measure the cell viability in silencing LINC00958 of GCs under oxidative stress (n = 5). (K) MitoTracker (red) was used to stain mitochondria, and mitochondrial morphology is counted (n = 5). Scale bar, 10 μm. (L) ATP levels were measured following LINC00958 knockdown in GCs under oxidative stress (n = 5). (M) Western blot was used to measure the expression of apoptosis-associated proteins in GCs. (N) Mitochondrial membrane potential (MMP, ΔΨm) was measured by the JC-1 assays (n = 5). Scale bar, 50 μm. (O) Apoptotic cells were measured by flow cytometry in GCs (n = 3). Data represent the mean ± SD. *, $P < 0.05$; **, $P < 0.01$; ***, $P < 0.001$. (For interpretation of the references to colour in this figure legend, the reader is referred to the Web version of this article.)

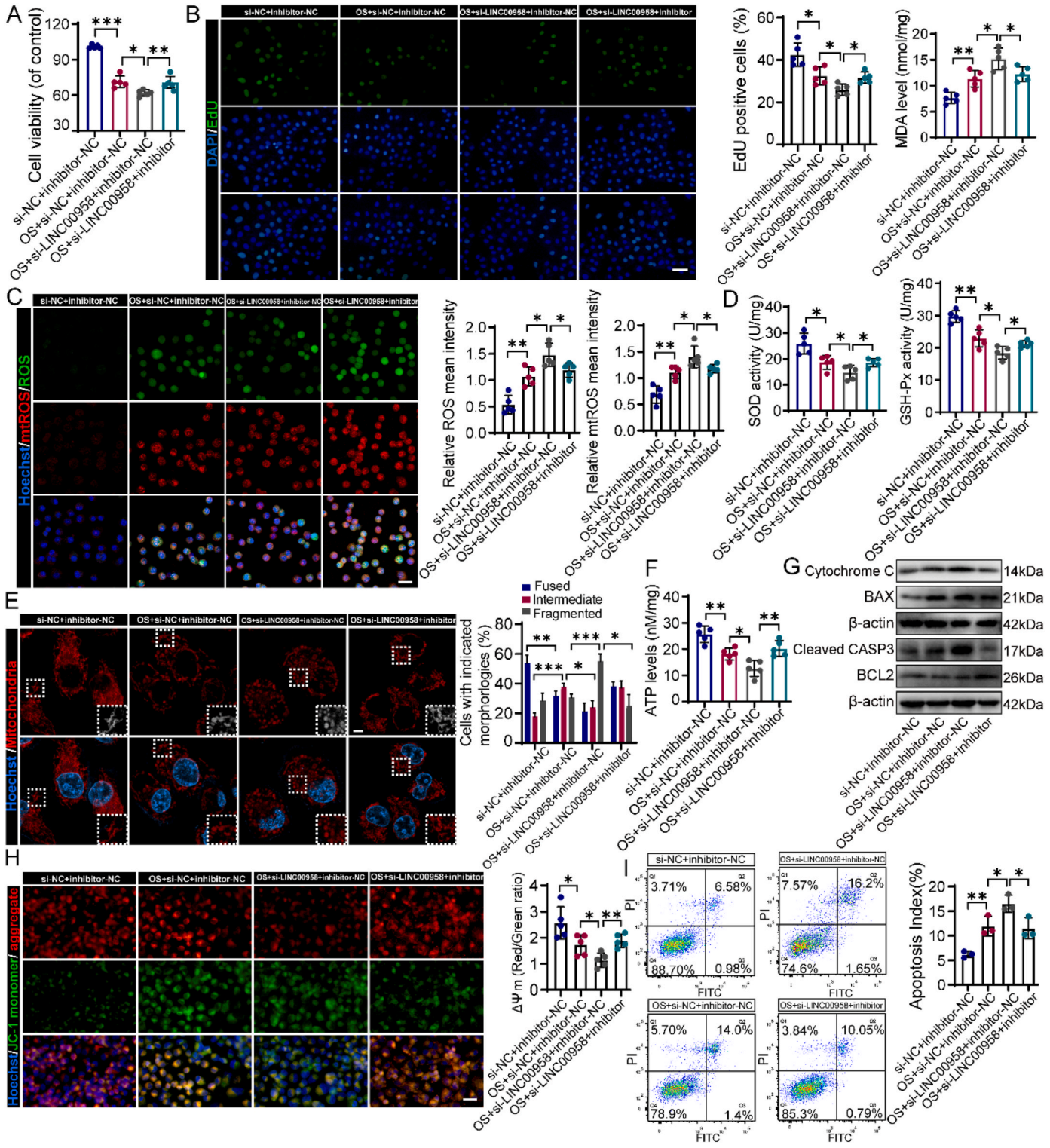

Fig. 4. Inhibiting miR-484 alleviated LINC00958 depletion-aggravated GC injuries under oxidative stress conditions. (A) Relative cell viability was measured by the CCK-8 assay (n = 5). (B) EdU assays of GCs and the percentage of EdU-positive GCs (Green) were measured (n = 5). Scale bar, 100 μm. (C) Cellular ROS (Green) and mtROS (Red) in GCs were assessed using DCFH-DA probe and MitoSOX Red mitochondrial superoxide indicator (n = 5). Scale bar, 50 μm. (D) The MDA level and total SOD and GSH-Px activities of GCs (n = 5). (E) MitoTracker (red) was used to stain mitochondria, and mitochondrial morphology is counted (n = 5). Scale bar, 10 μm. (F) ATP levels were measured (n = 5). (G) Western blot was used to measure the expression of apoptosis-associated proteins in GCs. (H) Mitochondrial membrane potential (MMP, ΔΨm) was measured by the JC-1 assays (n = 5). Scale bar, 50 μm. (I) Apoptotic cells were measured by flow cytometry in GCs (n = 3). Data represent the mean ± SD. *, $P < 0.05$; **, $P < 0.01$; ***, $P < 0.001$. (For interpretation of the references to colour in this figure legend, the reader is referred to the Web version of this article.)

D).

Given that miR-484 has been previously reported to be associated with mitochondrial fission and fusion [18], we next focused on the effect of miR-484 on mitochondrial functions. Under oxidative stress conditions, CGs transfected with exogenous miR-484 showed more mitochondrial fragments, increased MMP depolarization and reduced ATP levels (Fig. 2E, F, H). It seems that increased mitochondrial fragmentation can lead to mitochondrial depolarization, which is an early indicator of mitochondrial apoptosis, so we next investigated the impact of miR-484 overexpression or knockdown on GCs apoptosis. As expected, a much higher ratio of apoptotic GCs was observed after miR-484 overexpression (Fig. 2I), which was associated with increased cytochrome C release and dysregulated expression of mitochondrial apoptosis-related proteins including increased BAX, cleaved-caspase3 and reduced BCL2 (Fig. 2G, Fig. S4A). In contrast, an opposite trend was observed after miR-484 inhibition (Fig. 2G, I).

Endoplasmic reticulum (ER) stress and senescence-associated secretory phenotype (SASP) play important roles in the development and pathogenesis of human ovarian diseases, which occurred in ovarian cells, affecting oocyte maturation, follicle formation and ovulation [28–30]. Thus, we sought to determine whether miR-484 regulate oxidative stress-induced ER stress in GCs. We detected the ER morphological changes using ER-tracker and found that miR-484 mimic obviously increased fluorescence signals (Fig. S2H). The expression of ER stress marker genes and UPR sensor proteins was measured and miR-484 overexpression upregulated the mRNA expression level of GRP78, CHOP and XBP1s in GCS under oxidative stress conditions (Fig. S2J). Therefore, the effect of miR-484 to regulate the SASP was investigated analysing the expression levels of proinflammatory cytokines, such as IL-1β and IL-6, as shown in Fig. S2K, the expression and secretion of TNF, IL-6 and IL-1β as well as the expression of CCL2 were significantly increased in miR-484 overexpressed GCs. The opposite trend was observed in miR-484 depleted GCs.

Collectively, these data proved that miR-484 had a negative effect on GCs functions by disrupting mitochondrial networks and supplying a pro-apoptotic environment for GCs under oxidative stress conditions.

3.3. Prediction and confirmation of direct interaction between miR-484 and LINC00958 in GCs

It is well known that competing endogenous RNAs (ceRNA) can bind with microRNA through the response element (microRNA response elements, MREs). After screening in multiple prediction databases, we found 19 candidate lncRNAs, as shown in Fig. S3A. After the verification via RT-qPCR and FISH, it was speculated that LINC00958, which was significantly decreased in GCs under oxidative stress conditions, was the upstream ceRNA of miR-484 (Fig. 3A and Fig. S3B).

Subsequently, we used a dual luciferase reporter assay to verify this prediction. The luciferase signal of the LINC00958-WT reporter was suppressed by miR-484, whereas LINC00958-Mut abolished the inhibitory effect of miR-484 (Fig. 3B and C). As demonstrated in Fig. 3F and G, the results of AGO2-RIP-qPCR showed that LINC00958 and miR-484 was significantly enriched in the AGO2 IP sample compared to control IgG sample. Next, we analyzed the direct interaction between LINC00958 and miR-484 using RNA pull-down assay. Compared to the bio-NC pull-down group, LINC00958 was significantly higher in the bio-miR-484 pull-down group (Fig. 3D). Subsequently, biotin-labeled LINC00958 pull-down assays showed significantly increased miR-484

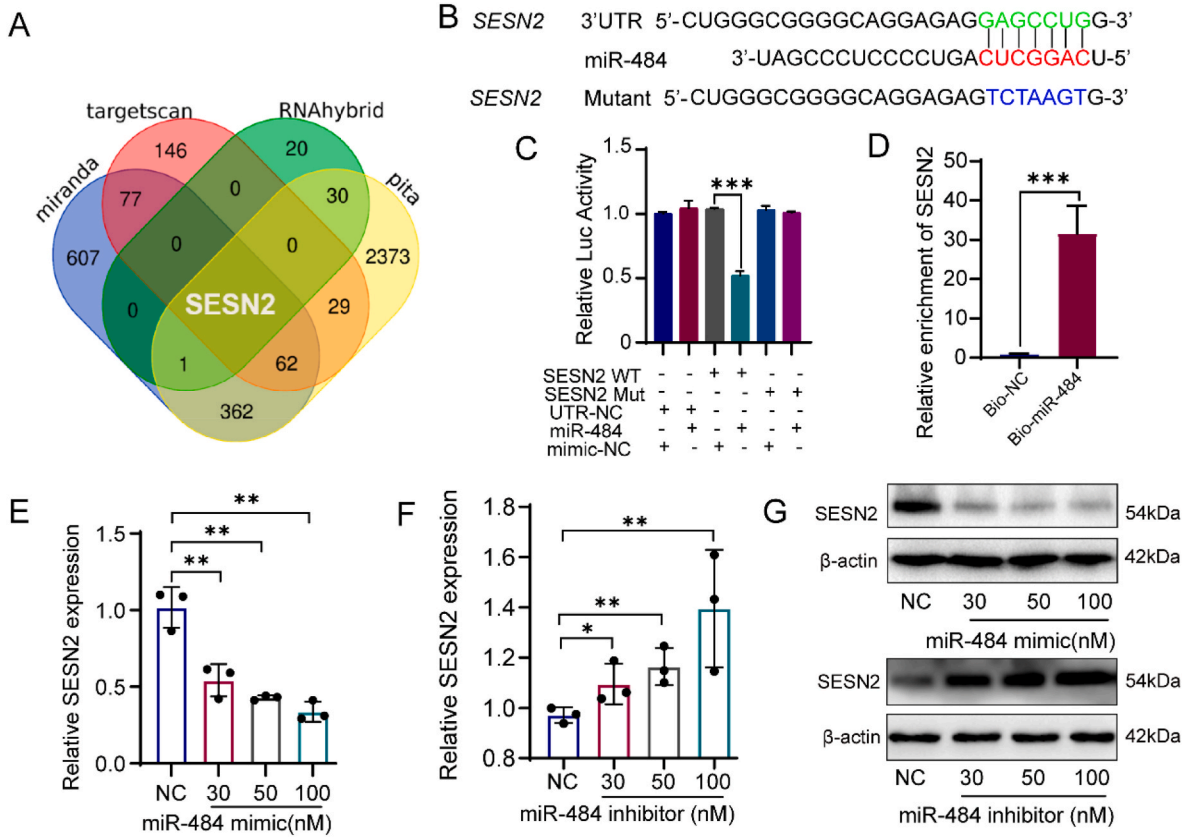

Fig. 5. Sestrin2(SESN2) is a direct downstream mRNA target of miR-484 in GCs. (A)Venn diagram showing predicted target gene of miR-484 by four algorithms (miRanda, TargetScan, RNAhybrid, and PITA). (B–C) Dual luciferase reporter analysis showed that miR-484 could bind to the 3′-UTR of SESN2. (D) Enrichment of SESN2 pulled down by biotin-miR-484 or negative control. (E–G) The mRNA and protein expression of SESN2 was decreased or increased in a dose-dependent manner when miR-484 overexpressed or knockdown by RT-qPCR and Western blot assays (n = 3). Data represent the mean ± SD. *, $P < 0.05$; **, $P < 0.01$; ***, $P < 0.001$.

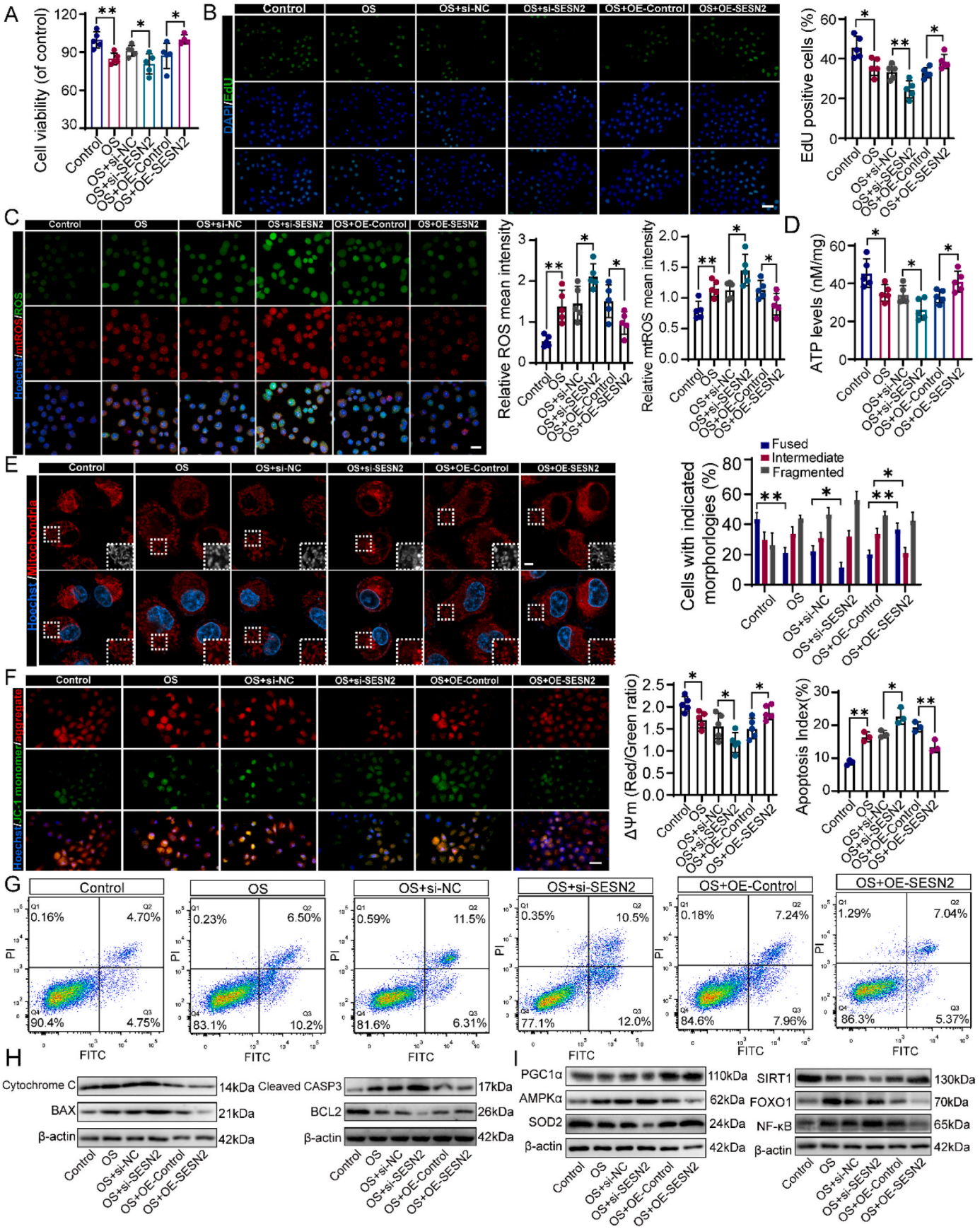

(caption on next page)

Fig. 6. SESN2 positively regulated GCs functions after oxidative stress injury. (A) CCK-8 assays were performed to measure the cell viability in silenced- or overexpressed-SESN2 in GCs under oxidative stress (n = 5). (B) EdU assays of GCs and the percentage of EdU-positive GCs (Green) were measured (n = 5). Scale bar, 100 μm. (C) Cellular ROS (Green) and mtROS (Red) in GCs were assessed using DCFH-DA probe and MitoSOX Red mitochondrial superoxide indicator (n = 5). Scale bar, 50 μm. (D) ATP levels were recorded following miR-484 knockdown or overexpression in GCs under oxidative stress (n = 5). (E) MitoTracker (red) was used to stain mitochondria, and mitochondrial morphology is counted (n = 5). Scale bar, 10 μm. (F) Mitochondrial membrane potential (MMP, ΔΨm) was measured by the JC-1 staining (n = 5). Scale bar, 50 μm. (G) Apoptotic cells were measured by flow cytometry in GCs (n = 3). (H) Western blot was used to measure the expression of apoptosis-associated proteins in GCs. (I) The protein expression levels of SESN2 downstream molecules and antioxidant related molecules. Data represent the mean ± SD. *, $P < 0.05$; **, $P < 0.01$; ***, $P < 0.001$. (For interpretation of the references to colour in this figure legend, the reader is referred to the Web version of this article.)

interaction in the GCs compared to that in the control, suggesting that there was a direct interaction between LINC00958 and miR-484 (Fig. 3E).

We next explored the role of LINC00958 in regulating GCs functions by transfecting GCs with LINC00958-directed siRNAs. As shown in Fig. S3C, si2-LINC00958 showed the most obvious silencing effect and was selected for the subsequent experiments. Meanwhile, the expression level of miR-484 significantly increased after LINC00958 silencing, whereas LINC00958 expression was obviously suppressed by overexpression of miR-484 mimic (Fig. S3E). The results of CCK-8 assays and EdU assays showed that Compared with the OS group treated with si-NC, the down-expression of LINC00958 significantly decreased the proliferation of GCs (Fig. 3H, J). Moreover, LINC00958 knockdown plus oxidative stress group resulted in higher oxidative stress injury in GCs than the OS group, as exhibited by the higher MDA content, less SOD and GSH-Px enzyme activities, and more enhanced expression of intracellular ROS and mtROS (Fig. 3I and Fig. S3G).

Furthermore, GCs displayed particularly fragmented mitochondrial networks after oxidative stress exposure, whereas more mitochondrial fragments were observed after si-LINC00958 transfection (Fig. 3K). Subsequently, silencing LINC00958 obviously worsened MMP depolarization and decreased ATP levels in GCs under oxidative stress conditions (Fig.3L, N). Accordingly, a much higher apoptotic rate was observed in GCs after LINC00958 deletion (Fig. 3O), which was consistent with increased mitochondrial apoptosis-related proteins, including BAX and cleaved-caspase3 (Fig.3M, Fig. S4B).

These results further confirmed that LINC00958 targeted miR-484 to act as a molecular sponge in GCs which played an important role in promoting GCs functions by balancing mitochondrial dynamics and inhibiting mitochondria-dependent apoptosis.

3.4. Inhibiting miR-484 alleviated LINC00958 depletion-aggravated GC injuries under oxidative stress conditions

Given that LINC00958 was identified as a molecular sponge of miR-484, further experiments were given to reveal the functional interactions between LINC00958 and miR-484. As shown in previous results, silencing LINC00958 exacerbated GC dysfunction under oxidative stress conditions, including impaired cell viability and proliferative ability (Fig. 4A and B). However, miR-484 inhibitor remarkably alleviated the negative effects of LINC00958 depletion, suggesting that miR-484 is a downstream target of LINC00958 with antagonistic functions (Fig. 4A and B). In addition, inhibiting miR-484 also alleviated the oxidative stress injury aggravated by LINC00958 silencing, as indicated by increased SOD and GSH-Px enzyme activities, decreased MDA contents and reduced cellular ROS and mtROS (Fig. 4C and D).

To further investigate the influence of miR-484 on LINC00958-mediated mitochondrial functions. Compared to that in GCs with silencing LINC00958, less mitochondrial fragments were found after miR-484 inhibitor treatment (Fig. 4E), which indicate that inhibiting miR-484 could moderate the imbalance between fission- and fusion after LINC00958 silencing. In addition, silencing miR-484 further suppressed MMP depolarization and increased ATP levels after LINC00958 inhibition (Fig. 4F, H). Furthermore, co-transfection with the miR-484 inhibitor reduced the proportion of apoptotic GCs (Fig. 4I), the release of cytochrome C, the increased protein expression of BAX and cleaved caspase3 and the reduction in BCL-2 compared with transfection with LINC00958 alone (Fig. 4G and Fig. S4C).

In summary, these data showed that LINC00958, an upstream regulator of miR-484, exerts the opposite effects to miR-484 in terms of oxidative stress and mitochondrial protection.

3.5. Sestrin2(SESN2) is a direct downstream mRNA target of miR-484 in GCs

To further investigate the ceRNA network connecting with LINC00958 and miR-484, we next attempted to identify the specific target mRNA of miR-484 in GCs under oxidative stress conditions.

According to the results of four different miRNA target prediction tools miRanda, TargetScan, RNAhybrid and PITA, SESN2 was the only overlapping target of miR-484 in GCs (Fig. 5A). Fig. 5B shows the fragments in the 3′UTR of SESN2 matching the seed sequence of miR-484 using TargetScan. These fragments were cloned into a reporter plasmid at the downstream of the luciferase coding sequence. The luciferase reporter assay showed that miR-484 had an inhibitory effect on the luciferase activities of the SESN2-WT reporters, whereas the luciferase activities remained unaffected when the binding sites were mutated (Fig. 5C).

Then, GCs were transfected with the miR-484 mimic or miR-484 inhibitor of different concentrations to elucidate whether miR-484 could regulate SESN2 expression at the transcriptional and translational levels. As shown in Fig. 5E and G, both the mRNA and protein levels of SESN2 were significantly reduced in a dose-dependent manner when miR-484 was overexpressed (Fig. 5E, G and Fig. S4D). In contrast, GCs gained enhanced SESN2 expression as the concentration of transfected miR-484 increased, which was demonstrated by the results of western blot and RT-qPCR analyses (Fig. 5F, G and Fig. S4E). In addition, the interaction between an avidin-biotin miR-484 and SESN2 also demonstrated that SESN2 could endogenously bind to miRNA-484 (Fig. 5D).

Taken together, these results confirmed that SESN2 was the downstream target of miR-484, which may play an important role in GCs under oxidative stress conditions.

3.6. SESN2 positively regulated GCs functions after oxidative stress injury

SESN2 is an important member of the Sestrins family, which is a group of highly conserved stress-induced proteins that protect cells from detrimental factors such as stress and aging through a variety of pathways. To further investigate the role of SESN2 plays in GCs under oxidative stress conditions, we performed SESN2 knockdown or overexpression in vitro. As shown in Fig. S3F, transfection of si2-SESN2 and OE-SESN2 plasmid were effective (Fig. S3F and Fig. S4F&G). Under oxidative stress conditions, cell viability and proliferative ability were obviously decreased (Fig. 6A and B), the effects of which were further aggravated after SESN2 knockout. By contrast, overexpression of SESN2 significantly reversed cell dysfunction (Fig. 6A and B). Then, SESN2 overexpression decreased the content of cellular ROS, mtROS and MDA, increased enzyme activities of SOD and GSH-Px, demonstrating the potential function of SESN2 in alleviating cell oxidative stress (Fig. 6C, Fig. S3H).

We next investigated the possible impact of SESN2 overexpression on

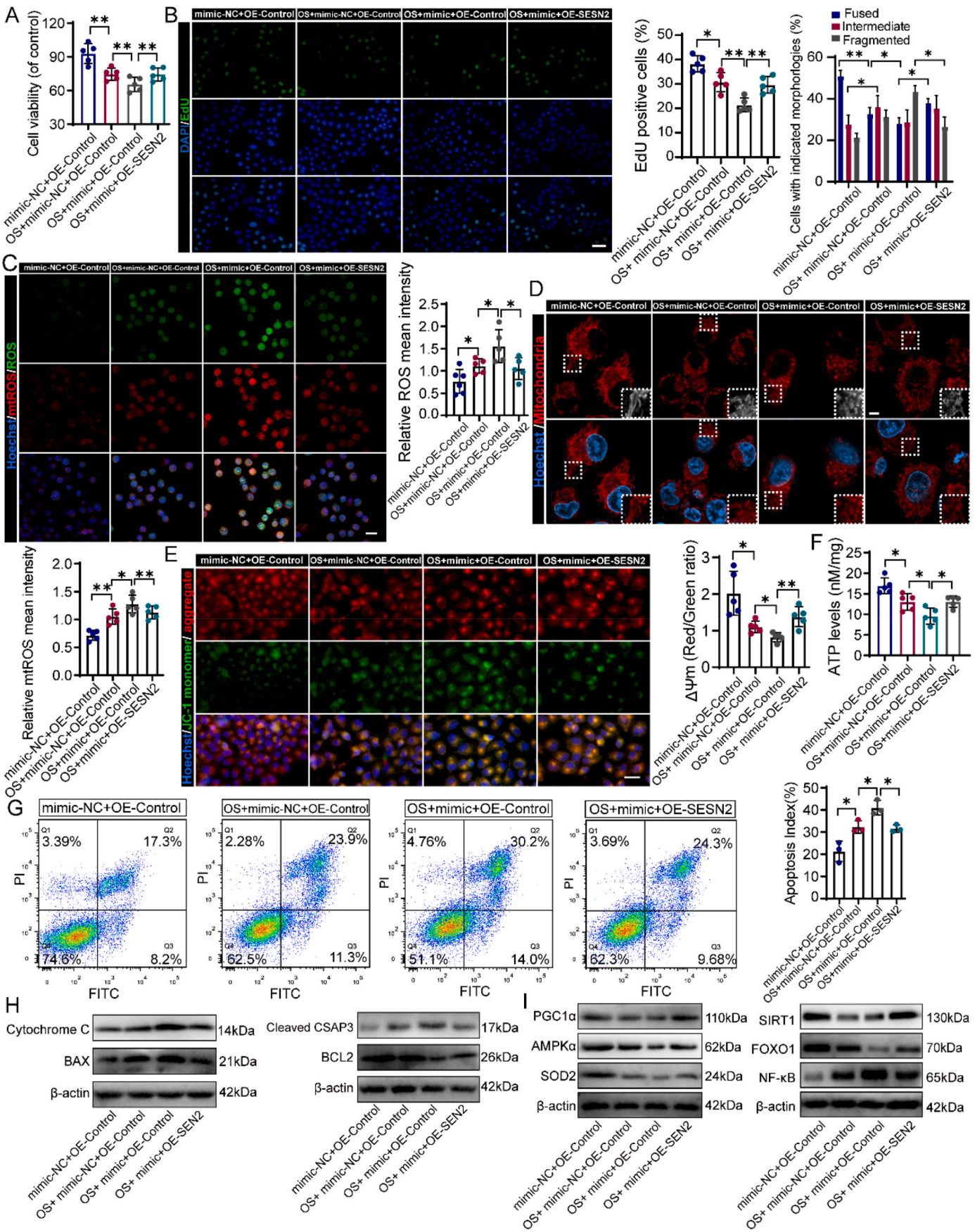

(caption on next page)

Fig. 7. SESN2 reversed miR-484 mediated mitochondrial damages and apoptosis in GCs under oxidative stress conditions. (A) Relative cell viability was measured by the CCK-8 assay (n = 5). (B) EdU assays of GCs and the percentage of EdU-positive GCs (Green) were measured (n = 5). Scale bar, 100 μm. (C) Cellular ROS (Green) and mtROS (Red) in GCs were assessed using DCFH-DA probe and MitoSOX Red mitochondrial superoxide indicator (n = 5). Scale bar, 50 μm. (D) MitoTracker (red) was used to stain mitochondria, and mitochondrial morphology is counted (n = 5). Scale bar, 10 μm. (E) Mitochondrial membrane potential (MMP, ΔΨm) was measured by the JC-1 assays (n = 5). Scale bar, 50 μm. (F) ATP levels were measured (n = 5). (G) Apoptotic cells were measured by flow cytometry in GCs (n = 3). (H) Western blot was used to measure the expression of apoptosis-associated proteins in GCs. (I) The protein expression levels of SESN2 downstream molecules and antioxidant related molecules. Data represent the mean ± SD. *, $P < 0.05$; **, $P < 0.01$; ***, $P < 0.001$. (For interpretation of the references to colour in this figure legend, the reader is referred to the Web version of this article.)

mitochondrial functions and mitochondrial apoptosis. Our results revealed that overexpression of SESN2 significantly reduced mitochondrial fragments, whereas an opposite trend was observed after SESN2 knockdown (Fig. 6E). Moreover, overexpression of SESN2 obviously inhibited MMP depolarization and increased ATP level, indicating that SESN2 overexpression alleviated mitochondrial dysfunction (Fig. 6D, F). In addition, flow cytometry analysis showed a remarkable decrease in the percentage of early and late apoptotic cells among the SESN2-overexpressed GCs after oxidative stress exposure (Fig. 6G). Moreover, SESN2 overexpression prevented cytochrome *c* being released from mitochondria, reduced BAX and cleaved caspase3 expression and increased BCL2 expression (Fig. 6H, Fig. S5A).

To gain greater insight into the function of SESN2 in GCs under oxidative stress conditions, we performed western blot analysis to examine the expression of downstream genes of SESN2. As shown in Fig. 6I, overexpression of SESN2 obviously upregulated AMPKα, FOXO1 and SIRT1. Furthermore, the levels of antioxidation-related molecules SOD2 and PGC1α were increased, whereas the level of NF-κB was downregulated after SESN2 overexpression (Fig. 6I, Fig. S5B).

Overall, these results confirmed that SESN2 was a downstream target of miR-484 and, to a large extent, was responsible for GCs recovery from oxidative stress related damages by regulating mitochondrial dynamics and suppressing apoptosis.

3.7. SESN2 reversed miR-484 mediated mitochondrial damages and apoptosis in GCs under oxidative stress conditions

To further illustrate whether SESN2 was involved in the regulatory processed of miR-484 mediated GCs dysfunction, we overexpressed SESN2 in the miR-484 mimic group based on our previous finding that overexpressing miR-484 further reduced SESN2 expression in GCs under oxidative stress conditions. Overexpression of SESN2 reversed the miR-484 mimic-induced reduction in cell viability and proliferative ability in GCs (Fig. 7A and B). In addition, exogenous overexpression of SESN2 remarkably alleviated oxidative stress in GCs transfected with miR-484 mimic, as indicated by higher MDA contents, higher SOD and GSH-Px enzyme activities and significantly suppressed intracellular ROS and mtROS production (Fig. 7C, Fig. S3I).

We next sought to demonstrate the potential role of SESN2 in oxidative stress and miR-484 overexpression-induced mitochondrial damages in GCs. As expected, SESN2 facilitated fragmented mitochondria to transform into filamentous ones, which indicates that the mitochondrial network was appropriately reconstructed (Fig. 7D). Additionally, SESN2 clearly inhibited miR-484 overexpression induced MMP depolarization and ATP reduction (Fig. 7E and F). Our previous results exhibited that SESN2 have an anti-apoptotic effect on GCs. Given that SESN2 is a downstream target of miR-484, SESN2 overexpression also decreased miR484-meditaed cell apoptosis under oxidative stress conditions, which could be attributed to, at least partially, its inhibitory effects on the mitochondrial apoptosis pathway, as demonstrated by the reduced cytochrome C release, decreased BAX and cleaved-caspase3 expression and increased BCL2 expression (Fig. 7Gand H, Fig. S5D).

We also detected that overexpression of SESN2 increased the expression of AMPKα、FOXO1 and SIRT1 (Fig. 7I). Furthermore, the expression of two other antioxidation-related proteins, SOD2 and PGC1α, was also strongly enhanced, whereas the level of NF-κB was downregulated by SESN2 overexpression (Fig. 7I and Fig. S5C).

In summary, these results indicated that SESN2 could be regulated by miR-484 and had a role in alleviating miR-484 overexpression-induced GCs dysfunction under oxidative stress conditions by ameliorating the disturbance of mitochondrial dynamics and apoptosis pathway.

3.8. Inhibition of miR-484 ameliorated ovarian oxidative stress injuries in mice

Based on the results that miR-484 is highly expressed in ovaries and GCs under oxidative stress conditions and inhibiting miR-484 can alleviate oxidative stress-induced cell injuries by improving mitochondrial functions and reducing GCs apoptosis (Fig. 1 and Fig. 2), we next tried to provide more evidence for the involvement of miR-484 in regulating GCs functions. We knocked down miR-484 in mouse ovaries using AAV-inhibitor by intra-ovarian injection. Since the efficiency of miRNA inhibitor is verified by the expression level of its target genes, we identified that miR-484 inhibitor vector has a high knockdown efficiency by RT-qPCR and Western blot assays (Fig. S6A) As shown in Fig. S6B, the optimal dose and time of AAV administration were determined through in vivo pre-experiments. The results showed that oxidative stress exposure did not result in any difference in body weight, but significantly decreased the ovary coefficient, reduces serum levels of estradiol, FSH, and AMH, and disturbed estrous cycle (Fig. S6C,D,E). In contrast, mice in the AAV-inhibitor group had a relatively regular estrous cycle, an elevated AMH level, increased primordial follicle counts and decreased atretic follicles, which were consistent with the results observed in the positive control group injected with melatonin (Fig. 8A, B, D and Fig. S6E).

Additionally, knockdown of miR-484 ameliorated oxidative damage, as shown by the decreased MDA content, increased SOD and GSH-Px enzyme activities and decreased ROS in ovaries (Fig. 8C, Fig. S6F). Then, we evaluated the function of GCs in ovary by TUNEL and Ki-67 staining. Compared to the AAV-vector group, apoptotic cells were decreased, Ki-67 positive cells were significantly increased in AAV-inhibitor group, indicating that inhibition of miR-484 inhibited apoptosis and promoted proliferation of GCs in ovarian oxidative stress conditions (Fig. 8E and F).

These data directly indicated that miR-484 inhibition can exert beneficial effects on GCs under ovarian oxidative stress conditions by alleviating apoptosis and promoting proliferation.

4. Discussion

The potential effects of miR-484 in regulating oxidative stress in GCs were identified in the present study. miR-484 was increased in 3-NP-induced oxidative stress models of ovaries and GCs. The overexpression of miR-484 aggravated cell dysfunction and thereby intensified ovarian oxidative stress injury in mice. The potential mechanisms could involve the downregulation of LINC00958 and its direct binding with SESN2 mRNA under oxidative stress conditions in GCs, which in turn damaged mitochondrial function and compromised the mitochondrial-related apoptosis signaling pathway in GCs (Fig. 9). At same time, the inhibition of miR-484 alleviated oxidative stress induced GCs dysfunction.

GCs constitute the largest cell population of ovarian follicles. Their metabolism and apoptosis are closely associated with ovary dysfunction [31,32]. Oxidative stress, which is one of the main causes of cell

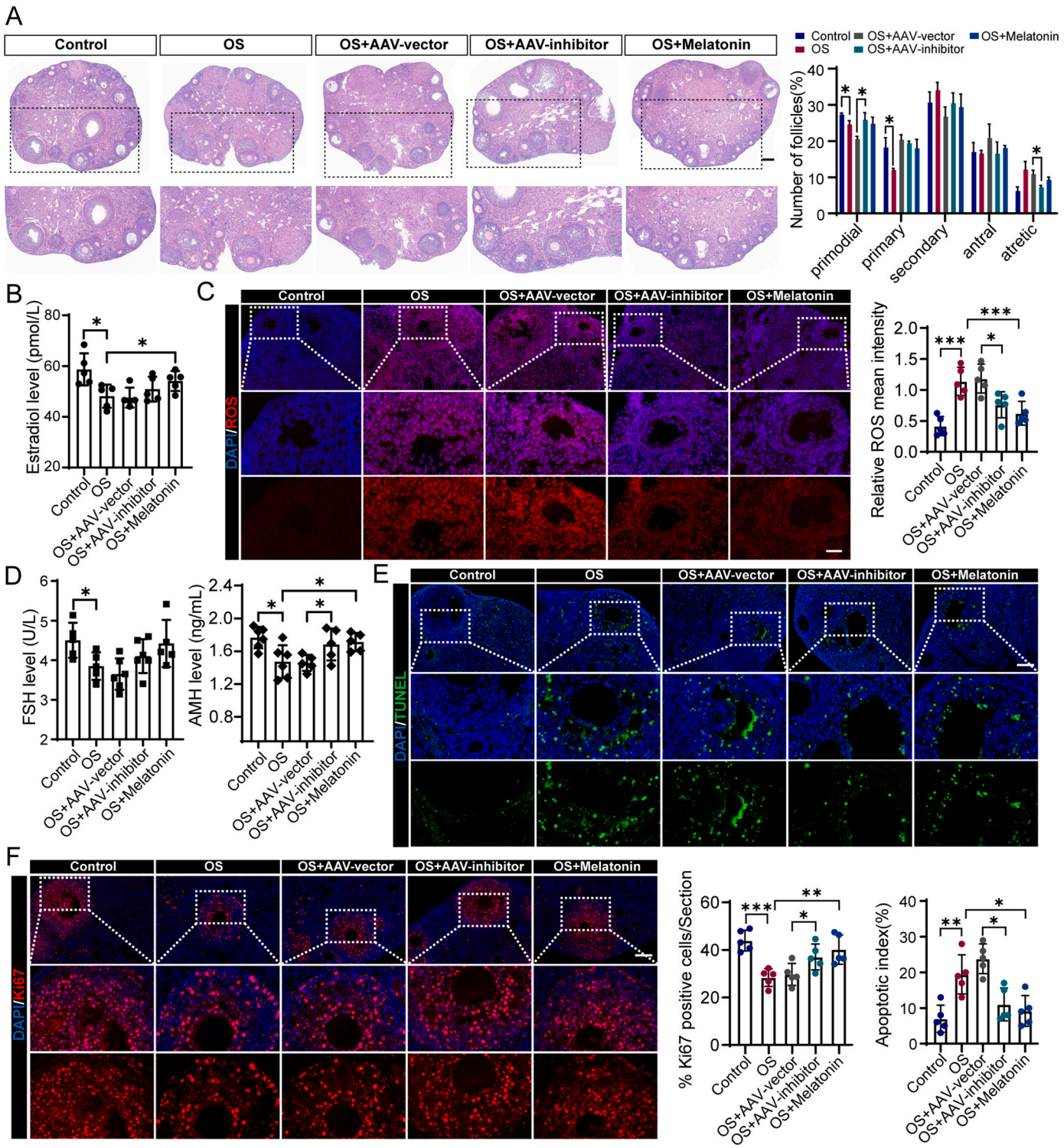

Fig. 8. Inhibition of miR-484 ameliorated ovarian oxidative stress injuries in mice. (A) H&E staining to show ovarian structures in the Control, OS, OS + AAV-vector, OS + AAV-inhibitor, and OS + Melatonin groups and the number of follicles was quantified for each group (n = 5). Scale bar,500 μm. (B, D) The level of estradiol, FSH and AMH of serum in each group (n ≥ 5). (C) Ovarian ROS levels of mice were measured using DHE probe in each group (n = 5). Scale bar, 50 μm(E) TUNEL staining of ovaries and the percentage of TUNEL-positive section (Green) were quantified(n = 5). Scale bar, 50 μm. (F) Ki-67 staining of ovaries and the proportion of Ki-67 positive cells were measured(n = 5). Scale bar, 50 μm. Data represent the mean ± SD. *, $P < 0.05$; **, $P < 0.01$; ***, $P < 0.001$. (For interpretation of the references to colour in this figure legend, the reader is referred to the Web version of this article.)

apoptosis, results from ROS overproduction and impaired antioxidant mechanism [33,34]. Under physiological conditions, age-related ROS accumulation drives GCs apoptosis. Meanwhile, ROS accumulation caused by intracellular factors (such as mitochondrial mutation, nutritional deprivation and local ischemia) and extracellular factors (including smoking, air pollution and electromagnetic radiation) can accelerate GCs apoptosis and lead to ovarian dysfunction, such as polycystic ovary syndrome (PCOS) and DOR [35–37]. Therefore, protecting GCs from oxidative stress damages are of great significance for the treatment of ovarian dysfunction and premature ovarian failure.

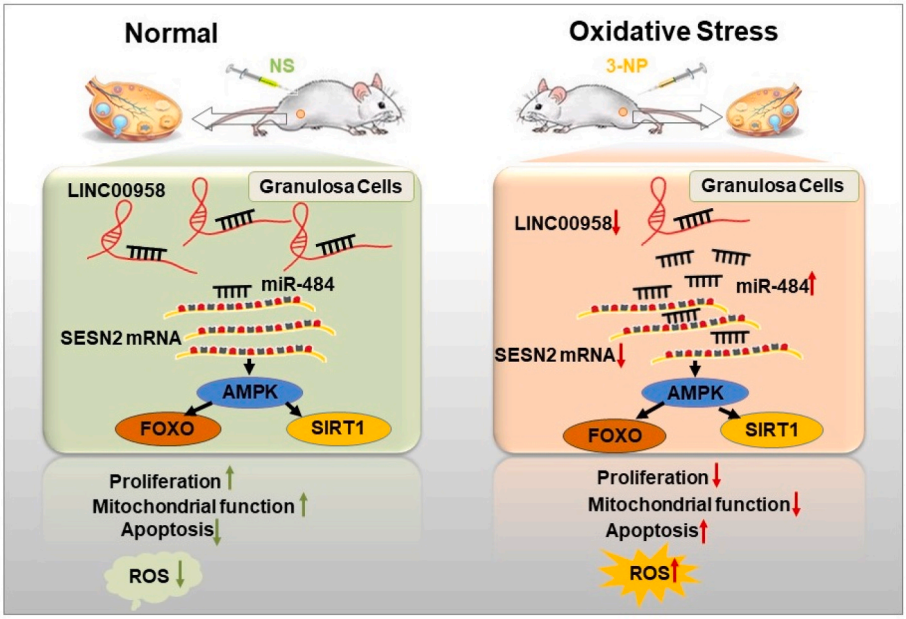

Fig. 9. Schematic diagram showing the role of miR-484 mediates oxidative stress-induced ovarian dysfunction by suppressing granulosa cell function via mitochondrial-related apoptosis.

With the in-depth study of miRNAs, the role of miRNA in ovaries has been gradually unveiling in recent years. It has been found that miRNA can regulate the development of ovarian follicles by affecting GCs proliferation [38], steroid hormone synthesis [39], oocyte maturation [40] and GCs functions. Gebremedhn et al. found that bovine miR-183-96-182 promoted the proliferation of ovarian GCs by synergistically targeting FOXO1 [41]. In addition, miR-17-92 promoted the proliferation of GCs and reduced the differentiation ratio of GCs by synergistically inhibiting the expression of PTEN and BMPR2 [42]. However, the role of miR-484 in regulating GCs apoptosis has not been reported yet.

In our previous study, miR-484 was found to be highly expressed in GCs of DOR patients and negatively correlated with the outcomes of assisted reproductive technology. Further exploration of underlying mechanisms showed that miR-484 could target YAP1 and participate in the pathogenesis of DOR [19]. The present study revealed that miR-484 is highly expressed in 3-NP-induced oxidative stress models of ovaries and GCs. In addition, bioinformatics analysis of the transcriptome sequencing results of 3NP-induced GCs showed that oxidative stress induced abnormal expression of several transcription factors regulating miR-484, among which the up-regulated transcription factors had higher fold changes (Fig. S7A-C). we found TFs related to chromosome remodeling and histone modification, such as EP300, TET2, KMT2D and KDM2B, among which EP300 was particularly associated with the Nrf2 pathway and identified as a co-activator of HIF1A. These results suggest that oxidative stress may induce some epigenetic changes that ultimately lead to miR-484 alteration. Overexpressing miR-484 compromised GCs function by damaging mitochondrial functions and increasing apoptosis under oxidative stress conditions, which were also mutually verified by previous studies. Moreover, miR-484 knockdown promoted GCs proliferation and decreased intercellular ROS contents after oxidative stress exposure. The potential mechanisms could be attributed to the possible role of miR-484 in regulating mitochondrial functions and the mitochondria-related apoptotic pathway.

Mitochondria are an important organelle of GCs not only for their functions in generating ATP but also for their role in transmitting extracellular and intracellular signals when GCs are exposed to environmental stress or injury [43,44]. Persistent mitochondrial dysfunction can lead to oxidative stress-induced damages in GCs, which will in turn result in increased apoptosis, reduced proliferation, impaired biological functions and aberrant follicular development or even ovarian disorders [45,46].

SESN2 is a member of the Sestrins protein family which plays a major role in many pathophysiological processes such as endoplasmic reticulum stress, hypoxia, oxidative stress and DNA damage, and has become a research focus recently [47]. SESN2 is not only a downstream antioxidant enzyme regulated by the Keap1/Nrf2/ARE signaling pathway, but also an upstream activator of the classical antioxidant pathway [48].It was found that cellular ROS accumulation upregulates SESN2, activates serine/threonine protein kinase, promotes phosphorylation of Beclin1 serine 14 site, which in turn binds to the ubiquitin ligase Parkin to promote selective autophagy in fragmented mitochondria [49]; SESN2 also mediates AMPK-PGC1α activation to promote mitochondrial biosynthesis, thereby reducing oxygen glucose depletion derived cellular damages [50]. It is evident that SESN2, as a highly conserved multifunctional protein, has a multifaceted regulatory role in anti-oxidative-stress processes and mitochondria-related regulation.

The ceRNA hypothesis is one of the mainstream views to explain how miRNAs function in various biological processes, revealing how LINC00958 affects the transcriptional process of its target mRNAs by directly sponging miR-484 through binding sites. And then, miR-484 represses the expression of its target mRNA SESN2 by binding the AGO2 protein to form RISC, where SESN2 mRNA will degrade. Herein, LINC00958 was predicted to be a specific molecular sponge of miR-484 and acted as an upstream regulatory factor of miR-484 and SESN2. Current studies on LINC00958 have mainly focused on its role in tumors, including hepatocellular carcinoma, bladder cancer and osteosarcoma [51–53]. However, there is no study has been performed to reveal the correlation between LINC00958 and ovarian reserve or GCs functions. In this study, we first demonstrated that LINC00958 is involved in regulating GCs functions after oxidative stress injury. First, we predicted and confirmed the direct interaction between miR-484 and LINC00958 in GCs. Functionally, the inhibition of miR-484 reversed the downregulation of LINC00958 under oxidative stress conditions and rebalanced the mitochondrial function and mitochondria-related apoptosis signaling. In Fig. S7D&E, bioinformatics analysis showed that oxidative stress induced downregulation of several transcription factors regulating LINC00958.

In summary, our study validated a new ceRNA network in remolding mitochondrial functions and GCs functions under oxidative stress conditions. Reducing LINC00958 activated miR-484 and subsequently decreased SESN2 expression, contributing to mitochondrial dysfunction and facilitating mitochondria-related apoptosis in GCs. miR-484 inhibition mediated mitochondrial homeostasis improves the resistance of GCs to oxidative stress injury and thereby enhances the prognosis of ovarian functions under oxidative stress conditions. Our findings provide a novel regulatory mechanism involved in regulating mitochondrial functions in GCs and form a theoretical basis for improving GCs functions and alleviating ovarian oxidative stress damages.

Funding statement

This work was supported by the National Key Research and Development Program of China (2022YFC2703000).

Author contributions

Conceptualization the project, Xiaofei, Wang; writing and performing the experiment, Xiaofei, Wang, Jiahao Yang, Huiying, Li, Hongbei Mu and Siying Cai; bioinformatics analysis, Ling Zeng and Ping Su; review and editing, Wenpei Xiang, Ling Zhang and Huaibiao Li.

Declaration of competing interest

No conflict of interest exits in the submission of this manuscript, and manuscript is approved by all authors for publication. I would like to declare on behalf of my co-authors that the work described was original research that has not been published previously, and not under consideration for publication elsewhere, in whole or in part. All the authors listed have approved the manuscript that is enclosed.

Data availability

Data will be made available on request.

Acknowledgements

The authors declare no conflict of interest.

Appendix A. Supplementary data

Supplementary data to this article can be found online at https://doi.org/10.1016/j.redox.2023.102684.

References

[1] L. Thurston, A. Abbara, W.S. Dhillo, Investigation and management of subfertility, J. Clin. Pathol. 72 (2019) 579–587, https://doi.org/10.1136/jclinpath-2018-205579.
[2] M.C. Magnus, A. Fraser, J.W. Rich-Edwards, P. Magnus, D.A. Lawlor, S.E. Haberg, Time-to-pregnancy and risk of cardiovascular disease among men and women, Eur. J. Epidemiol. 36 (2021) 383–391, https://doi.org/10.1007/s10654-021-00718-8.
[3] A. Lei, H. You, B. Luo, J. Ren, The associations between infertility-related stress, family adaptability and family cohesion in infertile couples, Sci. Rep. 11 (2021), 24220, https://doi.org/10.1038/s41598-021-03715-9.
[4] Z. Zhou, D. Zheng, H. Wu, R. Li, S. Xu, Y. Kang, Y. Cao, X. Chen, Y. Zhu, S. Xu, et al., Epidemiology of infertility in China: a population-based study, BJOG 125 (2018) 432–441, https://doi.org/10.1111/1471-0528.14966.
[5] R. Bala, V. Singh, S. Rajender, K. Singh, Environment, lifestyle, and female infertility, Reprod. Sci. 28 (2021) 617–638, https://doi.org/10.1007/s43032-020-00279-3.
[6] N.M. Crawford, A.Z. Steiner, Age-related infertility, Obstet. Gynecol. Clin. N. Am. 42 (2015) 15–25, https://doi.org/10.1016/j.ogc.2014.09.005.
[7] R.B. Gilchrist, M. Lane, J.G. Thompson, Oocyte-secreted factors: regulators of cumulus cell function and oocyte quality, Hum. Reprod. Update 14 (2008) 159–177, https://doi.org/10.1093/humupd/dmm040.
[8] E. Babayev, F.E. Duncan, Age-associated changes in cumulus cells and follicular fluid: the local oocyte microenvironment as a determinant of gamete quality, Biol. Reprod. 106 (2022) 351–365, https://doi.org/10.1093/biolre/ioab241.
[9] X. Liu, H. Mai, P. Chen, Z. Zhang, T. Wu, J. Chen, P. Sun, C. Zhou, X. Liang, R. Huang, Comparative analyses in transcriptome of human granulosa cells and follicular fluid micro-environment between poor ovarian responders with conventional controlled ovarian or mild ovarian stimulations, Reprod. Biol. Endocrinol. 20 (2022) 54, https://doi.org/10.1186/s12958-022-00926-1.
[10] L. Wang, J. Tang, L. Wang, F. Tan, H. Song, J. Zhou, F. Li, Oxidative stress in oocyte aging and female reproduction, J. Cell. Physiol. 236 (2021) 7966–7983, https://doi.org/10.1002/jcp.30468.
[11] A. Agarwal, S. Gupta, R.K. Sharma, Role of oxidative stress in female reproduction, Reprod. Biol. Endocrinol. 3 (2005) 28, https://doi.org/10.1186/1477-7827-3-28.
[12] X. Lin, Y. Dai, X. Tong, W. Xu, Q. Huang, X. Jin, C. Li, F. Zhou, H. Zhou, X. Lin, et al., Excessive oxidative stress in cumulus granulosa cells induced cell senescence contributes to endometriosis-associated infertility, Redox Biol. 30 (2020), 101431, https://doi.org/10.1016/j.redox.2020.101431.
[13] S. Prasad, M. Tiwari, A.N. Pandey, T.G. Shrivastav, S.K. Chaube, Impact of stress on oocyte quality and reproductive outcome, J. Biomed. Sci. 23 (2016) 36, https://doi.org/10.1186/s12929-016-0253-4.
[14] M. Saare, K. Rekker, T. Laisk-Podar, N. Rahmioglu, K. Zondervan, A. Salumets, M. Gotte, M. Peters, Challenges in endometriosis miRNA studies - from tissue heterogeneity to disease specific miRNAs, Biochim. Biophys. Acta, Mol. Basis Dis. 1863 (2017) 2282–2292, https://doi.org/10.1016/j.bbadis.2017.06.018.
[15] J.C. Eggers, V. Martino, R. Reinbold, S.D. Schafer, L. Kiesel, A. Starzinski-Powitz, A.N. Schuring, B. Kemper, B. Greve, M. Gotte, microRNA miR-200b affects proliferation, invasiveness and stemness of endometriotic cells by targeting ZEB1, ZEB2 and KLF4, Reprod. Biomed. Online 32 (2016) 434–445, https://doi.org/10.1016/j.rbmo.2015.12.013.
[16] J. He, B.H. Jiang, Interplay between reactive oxygen species and MicroRNAs in cancer, Curr. Pharmacol. Rep. 2 (2016) 82–90, https://doi.org/10.1007/s40495-016-0051-4.
[17] T. Liu, Y. Liu, Y. Huang, J. Chen, Z. Yu, C. Chen, L. Lai, miR-15b induces premature ovarian failure in mice via inhibition of alpha-Klotho expression in ovarian granulosa cells, Free Radic. Biol. Med. 141 (2019) 383–392, https://doi.org/10.1016/j.freeradbiomed.2019.07.010.
[18] K. Wang, B. Long, J.Q. Jiao, J.X. Wang, J.P. Liu, Q. Li, P.F. Li, miR-484 regulates mitochondrial network through targeting Fis1, Nat. Commun. 3 (2012) 781, https://doi.org/10.1038/ncomms1770.
[19] H. Li, X. Wang, H. Mu, Q. Mei, Y. Liu, Z. Min, L. Zhang, P. Su, W. Xiang, Mir-484 contributes to diminished ovarian reserve by regulating granulosa cell function via YAP1-mediated mitochondrial function and apoptosis, Int. J. Biol. Sci. 18 (2022) 1008–1021, https://doi.org/10.7150/ijbs.68028.
[20] M. Zhang, Q. Zhang, Y. Hu, L. Xu, Y. Jiang, C. Zhang, L. Ding, R. Jiang, J. Sun, H. Sun, et al., miR-181a increases FoxO1 acetylation and promotes granulosa cell apoptosis via SIRT1 downregulation, Cell Death Dis. 8 (2017) e3088, https://doi.org/10.1038/cddis.2017.467.
[21] X.Y. Shi, Z.Q. Guan, J.N. Yu, H.L. Liu, Follicle stimulating hormone inhibits the expression of p53 up-regulated modulator of apoptosis induced by reactive oxygen species through PI3K/Akt in mouse granulosa cells, Physiol. Res. 69 (2020) 687–694, https://doi.org/10.33549/physiolres.934421.
[22] J.Q. Zhang, M. Shen, C.C. Zhu, F.X. Yu, Z.Q. Liu, N. Ally, S.C. Sun, K. Li, H.L. Liu, 3-Nitropropionic acid induces ovarian oxidative stress and impairs follicle in mouse, PLoS One 9 (2014), e86589, https://doi.org/10.1371/journal.pone.0086589.
[23] X. Wang, M. Wang, L. Zeng, P. Su, Hypomethylation of LINE-1 retrotransposons is associated with cadmium-induced testicular injury, Environ. Sci. Pollut. Res. Int. 27 (2020) 40749–40756, https://doi.org/10.1007/s11356-020-10115-5.
[24] S.L. Byers, M.V. Wiles, S.L. Dunn, R.A. Taft, Mouse estrous cycle identification tool and images, PLoS One 7 (2012), e35538, https://doi.org/10.1371/journal.pone.0035538.
[25] Y.P. Hu, Y.P. Jin, X.S. Wu, Y. Yang, Y.S. Li, H.F. Li, S.S. Xiang, X.L. Song, L. Jiang, Y.J. Zhang, et al., LncRNA-HGBC stabilized by HuR promotes gallbladder cancer progression by regulating miR-502-3p/SET/AKT axis, Mol. Cancer 18 (2019) 167, https://doi.org/10.1186/s12943-019-1097-9.
[26] Y. Chen, S. Li, Y. Zhang, M. Wang, X. Li, S. Liu, D. Xu, Y. Bao, P. Jia, N. Wu, et al., The lncRNA Malat1 regulates microvascular function after myocardial infarction in mice via miR-26b-5p/Mfn1 axis-mediated mitochondrial dynamics, Redox Biol. 41 (2021), 101910, https://doi.org/10.1016/j.redox.2021.101910.
[27] H. Mu, S. Cai, X. Wang, H. Li, L. Zhang, H. Li, W. Xiang, RNA binding protein IGF2BP1 meditates oxidative stress-induced granulosa cell dysfunction by regulating MDM2 mRNA stability in an m(6)A-dependent manner, Redox Biol. 57 (2022), 102492, https://doi.org/10.1016/j.redox.2022.102492.
[28] M. Harada, N. Takahashi, J.M. Azhary, C. Kunitomi, T. Fujii, Y. Osuga, Endoplasmic reticulum stress: a key regulator of the follicular microenvironment in the ovary, Mol. Hum. Reprod. (2021) 27, https://doi.org/10.1093/molehr/gaaa088.
[29] S. Brenjian, A. Moini, N. Yamini, L. Kashani, M. Faridmojtahedi, M. Bahramrezaie, M. Khodarahmian, F. Amidi, Resveratrol treatment in patients with polycystic ovary syndrome decreased pro-inflammatory and endoplasmic reticulum stress markers, Am. J. Reprod. Immunol. 83 (2020), e13186, https://doi.org/10.1111/aji.13186.
[30] M.J. Schafer, X. Zhang, A. Kumar, E.J. Atkinson, Y. Zhu, S. Jachim, D.L. Mazula, A. K. Brown, M. Berning, Z. Aversa, et al., The senescence-associated secretome as an indicator of age and medical risk, JCI Insight (2020) 5, https://doi.org/10.1172/jci.insight.133668.
[31] H. Zhang, Q. Luo, X. Lu, N. Yin, D. Zhou, L. Zhang, W. Zhao, D. Wang, P. Du, Y. Hou, et al., Effects of hPMSCs on granulosa cell apoptosis and AMH expression and their role in the restoration of ovary function in premature ovarian failure

mice, Stem Cell Res. Ther. 9 (2018) 20, https://doi.org/10.1186/s13287-017-0745-5.
[32] D.B. Sreerangaraja Urs, W.H. Wu, K. Komrskova, P. Postlerova, Y.F. Lin, C. R. Tzeng, S.H. Kao, Mitochondrial function in modulating human granulosa cell steroidogenesis and female fertility, Int. J. Mol. Sci. (2020) 21, https://doi.org/10.3390/ijms21103592.
[33] A.K. Yadav, P.K. Yadav, G.R. Chaudhary, M. Tiwari, A. Gupta, A. Sharma, A. N. Pandey, A.K. Pandey, S.K. Chaube, Autophagy in hypoxic ovary, Cell. Mol. Life Sci. 76 (2019) 3311–3322, https://doi.org/10.1007/s00018-019-03122-4.
[34] Y. Gong, S. Luo, P. Fan, H. Zhu, Y. Li, W. Huang, Growth hormone activates PI3K/Akt signaling and inhibits ROS accumulation and apoptosis in granulosa cells of patients with polycystic ovary syndrome, Reprod. Biol. Endocrinol. 18 (2020) 121, https://doi.org/10.1186/s12958-020-00677-x.
[35] M. Huang, M. Huang, X. Li, S. Liu, L. Fu, X. Jiang, M. Yang, Bisphenol A induces apoptosis through GPER-dependent activation of the ROS/Ca(2+)-ASK1-JNK pathway in human granulosa cell line KGN, Ecotoxicol. Environ. Saf. 208 (2021), 111429, https://doi.org/10.1016/j.ecoenv.2020.111429.
[36] Y. Shi, H. Wang, M. Zheng, W. Xu, Y. Yang, F. Shi, Ginsenoside Rg3 suppresses the NLRP3 inflammasome activation through inhibition of its assembly, Faseb. J. 34 (2020) 208–221, https://doi.org/10.1096/fj.201901537R.
[37] X.H. Li, H.P. Wang, J. Tan, Y.D. Wu, M. Yang, C.Z. Mao, S.F. Gao, H. Li, H. Chen, W.B. Cai, Loss of pigment epithelium-derived factor leads to ovarian oxidative damage accompanied by diminished ovarian reserve in mice, Life Sci. 216 (2019) 129–139, https://doi.org/10.1016/j.lfs.2018.11.015.
[38] H.O. Pande, D. Tesfaye, M. Hoelker, S. Gebremedhn, E. Held, C. Neuhoff, E. Tholen, K. Schellander, D.S. Wondim, MicroRNA-424/503 cluster members regulate bovine granulosa cell proliferation and cell cycle progression by targeting SMAD7 gene through activin signalling pathway, J. Ovarian Res. 11 (2018) 34, https://doi.org/10.1186/s13048-018-0410-3.
[39] F.X. Donadeu, J.M. Sanchez, B.T. Mohammed, J. Ioannidis, C. Stenhouse, M. A. Maioli, C.L. Esteves, P. Lonergan, Relationships between size, steroidogenesis and miRNA expression of the bovine corpus luteum, Theriogenology 145 (2020) 226–230, https://doi.org/10.1016/j.theriogenology.2019.10.033.
[40] P.C. Au, S. Frankenberg, L. Selwood, M. Familari, A novel marsupial pri-miRNA transcript has a putative role in gamete maintenance and defines a vertebrate miRNA cluster paralogous to the miR-15a/miR-16-1 cluster, Reproduction 142 (2011) 539–550, https://doi.org/10.1530/REP-11-0208.
[41] S. Gebremedhn, D. Salilew-Wondim, M. Hoelker, F. Rings, C. Neuhoff, E. Tholen, K. Schellander, D. Tesfaye, MicroRNA-183-96-182 cluster regulates bovine granulosa cell proliferation and cell cycle transition by coordinately targeting FOXO1, Biol. Reprod. 94 (2016) 127, https://doi.org/10.1095/biolreprod.115.137539.
[42] E. Andreas, M. Hoelker, C. Neuhoff, E. Tholen, K. Schellander, D. Tesfaye, D. Salilew-Wondim, MicroRNA 17-92 cluster regulates proliferation and differentiation of bovine granulosa cells by targeting PTEN and BMPR2 genes, Cell Tissue Res. 366 (2016) 219–230, https://doi.org/10.1007/s00441-016-2425-7.
[43] D.A. Chistiakov, T.P. Shkurat, A.A. Melnichenko, A.V. Grechko, A.N. Orekhov, The role of mitochondrial dysfunction in cardiovascular disease: a brief review, Ann. Med. 50 (2018) 121–127, https://doi.org/10.1080/07853890.2017.1417631.
[44] R.Z. Zhao, S. Jiang, L. Zhang, Z.B. Yu, Mitochondrial electron transport chain, ROS generation and uncoupling (Review), Int. J. Mol. Med. 44 (2019) 3–15, https://doi.org/10.3892/ijmm.2019.4188.
[45] Y. Wang, Q. Yang, H. Wang, J. Zhu, L. Cong, H. Li, Y. Sun, NAD+ deficiency and mitochondrial dysfunction in granulosa cells of women with polycystic ovary syndromedouble dagger, Biol. Reprod. 105 (2021) 371–380, https://doi.org/10.1093/biolre/ioab078.
[46] Y. Wang, N. Li, Z. Zeng, L. Tang, S. Zhao, F. Zhou, L. Zhou, W. Xia, C. Zhu, M. Rao, Humanin regulates oxidative stress in the ovaries of polycystic ovary syndrome patients via the Keap1/Nrf2 pathway, Mol. Hum. Reprod. (2021) 27, https://doi.org/10.1093/molehr/gaaa081.
[47] C.L. Rytz, V. Pialoux, M. Mura, A. Martin, D.B. Hogan, M.D. Hill, M.J. Poulin, Impact of aerobic exercise, sex, and metabolic syndrome on markers of oxidative stress: results from the Brain in Motion study, J. Appl. Physiol. 2020 (128) (1985) 748–756, https://doi.org/10.1152/japplphysiol.00667.2019.
[48] B.Y. Shin, S.H. Jin, I.J. Cho, S.H. Ki, Nrf2-ARE pathway regulates induction of Sestrin-2 expression, Free Radic. Biol. Med. 53 (2012) 834–841, https://doi.org/10.1016/j.freeradbiomed.2012.06.026.
[49] X.Y. Zhang, X.Q. Wu, R. Deng, T. Sun, G.K. Feng, X.F. Zhu, Upregulation of sestrin 2 expression via JNK pathway activation contributes to autophagy induction in cancer cells, Cell. Signal. 25 (2013) 150–158, https://doi.org/10.1016/j.cellsig.2012.09.004.
[50] S.H. Ro, M. Nam, I. Jang, H.W. Park, H. Park, I.A. Semple, M. Kim, J.S. Kim, H. Park, P. Einat, et al., Sestrin2 inhibits uncoupling protein 1 expression through suppressing reactive oxygen species, Proc. Natl. Acad. Sci. U. S. A. 111 (2014) 7849–7854, https://doi.org/10.1073/pnas.1401787111.
[51] X. Zuo, Z. Chen, W. Gao, Y. Zhang, J. Wang, J. Wang, M. Cao, J. Cai, J. Wu, X. Wang, M6A-mediated upregulation of LINC00958 increases lipogenesis and acts as a nanotherapeutic target in hepatocellular carcinoma, J. Hematol. Oncol. 13 (2020) 5, https://doi.org/10.1186/s13045-019-0839-x.
[52] H. Zhen, P. Du, Q. Yi, X. Tang, T. Wang, LINC00958 promotes bladder cancer carcinogenesis by targeting miR-490-3p and AURKA, BMC Cancer (2021) 21–1145, https://doi.org/10.1186/s12885-021-08882-6.
[53] Y. Zhou, T. Mu, LncRNA LINC00958 promotes tumor progression through miR-4306/CEMIP axis in osteosarcoma, Eur. Rev. Med. Pharmacol. Sci. 25 (2021) 3182–3199, https://doi.org/10.26355/eurrev_202104_25727.